Environ. Sci. Technol. **2000**, *34,* 1636−1646

Chemical Characterization of a Chelator-Treated Soil Humate by Solution-State Multinuclear Two-Dimensional NMR with FTIR and Pyrolysis-GCMS

TERESA W.-M. FAN,*,† RICHARD M. HIGASHI,‡ AND ANDREW N. LANE§

Department of Land, Air & Water Resources and Crocker Nuclear Laboratory, University of California, One Shields Avenue, Davis, California 95616-8627, and Division of Molecular Structure, National Institute for Medical Research, The Ridgeway, Mill Hill, London NW7 1AA, U.K.

A California forest soil used for contaminant bioavailability studies was extracted for humic substances (HS) and then treated with 4,5-dihydroxy-1,3-benzene disulfonate ("Tiron") to remove exchangeable metal ions. This yielded HS that was readily water-soluble at neutral pH without residual Tiron contamination, and the gel electrophoretic pattern was very similar to an international reference HS. The improved solubility facilitated analysis of HS by solution-state 1-D and 2-D ^{1}H, ^{13}C, ^{31}P, and ^{13}C-^{1}H NMR. The amino acids Gly, Ala, Leu, Ile, Val, Asp, Ser, Thr, Glu, and Pro were identified in intact HS as peptidic from scalar coupling in TOCSY and dipolar interactions in NOESY and then confirmed by acid digestion of HS with 2-D ^{1}H NMR and GCMS analysis. The presence of peptides was also corroborated by FT-IR and pyrolysis-GCMS results. Carbohydrates containing α- and β-pyranoses, methoxy-phenylpropanyl structures, phosphate mono/diesters, polyphosphates, plus phosphatidic acid esters were also evident. Furthermore, the ^{1}H NOESY, TOCSY, and HSQC together indicated that the peptidic side chains were mobile, whereas aromatic groups were relatively rigid. Thus the peptidic moieties may be more readily accessible to aqueous contaminants than aromatic groups.

Introduction

Humic substances (*1*) (HS) are structurally diverse, primarily organic components of soils and sediments, which are formed through a wide variety of biogenic and abiotic reactions. They are heterogeneous in terms of elemental composition, chemical functionality (e.g. nonpolymeric nature), and molecular size distribution (e.g. polydisperse nature). This is because soil HS can be derived from any, or even all, organic materials, including plant and animal debris, microfauna, biowastes, pesticides, etc. Soil HS may also be cross-linked to inorganic ions and/or mineral matrix. Moreover, different humic components have the tendency to aggregate, which give rise to their colloidal properties. These complexities have been major challenges to the structural characterization of HS, which in turn hampered a molecular-level understanding of vital humic functioning in the environment. The latter include the roles of HS in plant growth and mineral nutrition, plant-microbe symbiosis, microbial metabolism and community, organic nutrition, and formation of soil aggregates as well as contaminant transport and bioavailability (*1*−*3*).

Despite the complexities, it is expected, and has been reported, that HS from different sources share some chemical commonality. For example, lignaceous and proteinaceous moieties are often reported as part of the HS structures (*4*−*6*), as are carbohydrate and lipid-type chemical groups (*7*). Moreover, isolated HS are typically polyanions rich in carboxylate groups (*7*) with charge densities higher than HS attached to soil (*8*), which can account for their high affinity for di- and trivalent metal ions. This makes it important to remove exchangeable metal ions from HS preparations, since they may be artifacts of the isolation procedure and can interfere with spectroscopic analysis.

An array of analytical approaches has been applied to humic structure characterization including chemical degradation, UV−visible spectrophotometry, fluorescence spectrophotometry, FT-IR, and pyrolysis GCMS as well as solid- and solution-state NMR (*3, 7*). Together, these techniques provide independent support for humic chemical groups while revealing different aspects of the humic structures. Among these methods, NMR spectroscopy has arguably provided the most interpretable information on the nature and relative abundance of chemical groups present in HS.

Solid-state ^{13}C NMR, in particular, has been the technique of choice for the analysis of intact HS in situ in soils and in isolated fractions (*5*). The chemical group assignment is primarily based on the range of ^{13}C chemical shifts observed in 1-D spectra by reference to those of known compounds. However, the chemical shift ranges for different chemical groups often overlap, which leads to uncertainty in the NMR assignment using the 1-D NMR approach alone. In addition, the ^{13}C NMR spectra of HS are usually crowded with a large number of broad resonances, which complicates the chemical group assignment. These problems are even more severe for solid-state ^{1}H NMR due to the smaller spectral range and very broad lines resulting from the strong dipolar coupling of protons in the solid-state (*9*). Thus, despite the much higher intrinsic sensitivity, solid-state ^{1}H NMR has very limited applications in HS analysis. Moreover, the 1-D approach is limited to providing clues on chemical groups rather than more extended molecular structures.

The situation is different for solution-state NMR. On one hand, the often low aqueous solubility of HS preparations and line broadening effects of the paramagnetic ions associated with HS have restricted the progress in solution-state ^{13}C NMR. On the other hand, solution-state ^{1}H NMR is much less affected by the dipolar line broadening that severely deteriorates the solid-state spectrum, while its superior sensitivity greatly reduces the solubility requirement for HS. More importantly, the recent literature has exploded with multidimensional ^{1}H NMR methods that have been developed for biomacromolecular structure studies (*10, 11*), which should be directly applicable to HS analysis. The advantages of multidimensional NMR over 1-D methods lie in the much improved spectral resolution and capability of providing information such as ^{1}H covalent network (e.g. TOCSY), ^{1}H-^{13}C or ^{1}H-^{15}N linkages (e.g. HSQC), spatial configuration (NOESY), and exchange dynamics (exchange spectroscopy). These 2-D NMR parameters not only minimize

* Corresponding author phone: (530)752-1450; fax: (530)752-1552; e-mail: twfan@ucdavis.edu.
† Department of Land, Air & Water Resources.
‡ Crocker Nuclear Laboratory.
§ National Institute for Medical Research.

10.1021/es991127v CCC: $19.00

Published on Web 03/30/2000

the ambiguities inherent in chemical shift-based assignment of chemical groups but also greatly facilitate the determination of structures and conformations of extended molecular fragments present in complex macromolecules. A few recent studies have begun to take the advantage of 2-D ^{1}H nuclear Overhauser effect spectroscopy (NOESY) for probing the solution conformation of soil HS (*12*) and the interaction between soil HS and important rhizosphere ligands such as bacteriosiderophores (*13*).

In this study, the source of HS is "Tinker" forest soil which has been employed extensively in studies on hydrophobic contaminant bioavailability (*14, 15*) and organic matter structural motifs by pyrolysis-GCMS and FT-IR spectroscopy (*16*). In addition to these whole soil studies, we are investigating the HS-ligand interaction properties (*13*), all for which HS structure information is paramount. Here, we used the metal chelator, 4,5-dihydroxy-1,3-benzene disulfonate (Tiron), to remove exchangeable metal ions from soil HS preparations such that the apparent HS solubility in water was improved (*17*). This, in turn, eliminated the use of strong base, strong acids such as HF, undesirable solvents such as DMSO, or selective fractionation through resins, thereby yielding in relatively few steps a product closer to whole HS. An extensive characterization of this product was conducted using a microsample energy-dispersive X-ray fluorescence (ED-XRF) method, C/N analyzer, peptide gel electrophoresis, FTIR, and pyrolysis-GCMS. This information was used to help interpret 2-D ^{1}H and ^{13}C-edited ^{1}H NMR as well as 1-D ^{31}P NMR analyses in terms of the primary structure of Tinker HS. Insights to the higher-order structure was also obtained, which has implications to contaminant binding or bioavailability properties (*14, 15*).

Materials and Methods

Humic Extraction from Soils. Humic substance (HS) was isolated from "Tinker" soil collected from 0 to 10 cm depth at a forested site of approximately 1680 m elevation, N39°19′ W120°36′ in the Sierra Nevada mountains, CA (*14, 15*). The soil was classified as a loamy-skeletal, mixed, mesic, typic durumbrept consisting of 0.19% in N, 4.3% in C, and 80.3% in ash (*16*). HS was extracted in He purged-NaOH (0.25 M) at 10 °C with rigorous shaking overnight, followed by centrifugation and filtration of the supernatant through a 0.45 μm cellulosic filter (modified from ref *18*). The extraction was repeated once, the supernatants were pooled, adjusted to pH 2 with concentrated HCl to precipitate HS, and centrifuged, and the resulting pellet was washed successively in 0.2 and 0.01 N HCl and lyophilized. The lyophilized powder was then extracted in 0.15 M 4,5-dihydroxy-1,3-benzene disulfonate (Tiron, Sigma Chemical Co., St. Louis, MO) at pH 6.3 and 35 °C for 24 h, followed by extensive wash with 0.01 N HCl to remove Tiron, as previously described (*13, 17*).

Energy-Dispersive X-ray Fluorescence (ED-XRF) and C/N Analyses. The Tiron-treated Tinker HS was analyzed by ED-XRF using a modified "microsample" XRF procedure (*19*) so that elemental analysis could be performed on small amounts of humic samples, at lower limits of detection. The HS powder was dissolved in doubly deionized water at 5 mg/mL, and a 10 μL aliquot (50 μg of HS) was mixed with 10 μL of 0.1 M sucrose before deposition onto a 4 μm thick low-metal polypropylene membrane (Ultralene membrane, Spex, NJ) and dried overnight under vacuum to result in a thin-film spot. The presence of sucrose facilitated adhesion of the spot to the membrane and limited the spread since the HS solution had high surfactant activity. The final HS spot was thus controlled by the procedure to be <6 mm in diameter to ensure that the entire sample was presented to the X-ray beam (collimated to 7 mm sample irradiation diameter). A set of five standards, consisting of mixtures of analytical reference solutions of the elements in Table 1 (Fisher Scientific, Pittsburgh, PA), was prepared by mixing each standard in equal volume with the Tinker HS+sucrose solution and spotted similarly as described above. The presence of Tinker HS in standards helped minimize matrix differences between the HS samples and standards. ED-XRF measurements were made using a JVAR (Austin, TX) EX-3600 XRF spectrometer with an organic window Li-drifted Si detector for better performance for low atomic number elements, run under vacuum with no filter, Rh anode X-ray tube set to 50 kV at amperage to achieve optimal dead time (approximately 45%, which was usually about 290 μA), spectral range of 40 keV, and live time acquisition of 1000 s. Using these conditions, elements of atomic number from Mg through U were measured simultaneously, with the exception of Cl, Ru, Rh, Pd, and Cd which, in practice, suffered interference from the unfiltered Rh anode X-ray. The correlation coefficients for the standard curves (five points) were >0.96. Duplicate HS samples were prepared and measured twice along with the set of standard-spiked HS. The C/N analysis and natural abundance isotope ratio determination was performed on 1−2 mg of Tinker HS by the UC Davis Stable Isotope Facility using a PDZ-Europa ANCA elemental analyzer interfaced to a PDZ Europa 20-20 continuous flow isotope ratio mass spectrometer.

TABLE 1. Elemental Profile of Tiron-Treated Tinker HS[a]

element[b]	mmol/g	SD (mmol/g)	% of HS	SD (%)
C[c]	42.24	0.74	50.69	0.89
N[c]	1.66	0.01	2.32	0.01
Al	1.24	0.37	3.35	1.00
P	0.68	0.21	2.10	0.65
S	0.60	0.06	1.94	0.18
K	0.70	0.01	2.75	0.05
Ca	0.45	0.02	1.80	0.09
Mn	0.29	0.02	1.59	0.10
Fe	0.33	0.01	1.85	0.07
Ni	0.21	0.01	1.25	0.07
Cu	0.21	0.01	1.36	0.09
Zn	0.18	0.01	1.16	0.06
Sr	0.13	0.01	1.15	0.05
Mo	0.15	0.00	1.47	0.03
total			74.78	3.32

[a] Na, Si, and Cl were present in significant amounts but were not quantified. [b] All other elements Mg through U (except Cl, Ru, Rh, Pd, and Cd due to X-ray tube interferences), including those sometimes found in soil such as Ti, V, Cr, Se, As, Br, and Ba, were below detectable limits. [c] Measured using the C/N analyzer, while the rest were analyzed by ED-XRF.

Ash Determination. Ash content of Tinker HS was determined using a CDS Pyroprobe 2000 microfurnace (CDS Analytical, Oxford, PA) at 550 °C and quartz tubes as crucibles. This temperature was chosen because ashing of the parent Tinker soil at 550 °C gave comparable results with the oxidizable carbon (C/N) analysis while exhibiting minimal loss of mineral spectral features as determined by FT-IR (*16*).

Sodium Dodecyl Sulfate Polyacrylamide Gel Electrophoresis (SDS-PAGE). The Tiron-treated HS preparation and soil humic standard of the International Humic Substances Society (IHSS) was dissolved in doubly deionized water, mixed with an equal volume of BioRad sample buffer, and electrophoresed in a polyacrylamide gel with the following compositions: 12.5% total acrylamide, 1.5% bisacrylamide, 4.6 M urea, 0.76 M Tricine, and 0.076% SDS for the separating gel plus 4% total acrylamide, 0.48% bisacrylamide, 0.31 M Tricine, and 0.033% SDS for the stacking gel (adapted from Schagger and von Jagow, 1987 (*20*)). The gel was then fixed in 70% methanol for 1 h, washed in 10% ethanol plus 5% acetic acid for 1 h, and stained in alcian blue (*21*) or Coomassie blue G-250 (BioRad protocol).

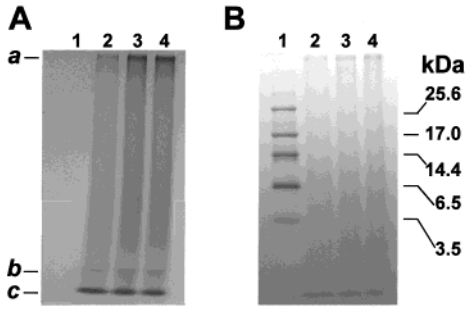

FIGURE 1. SDS-PAGE of Tiron-treated Tinker HS and IHSS HS standard. The SDS-PAGE was performed in Tricine-SDS buffer as described in Materials and Methods. Tinker HS (50 μg each in lanes 3 and 4) was electrophoresed along with IHSS HS (97 μg in lane 2) and peptide standards from BioRad (lane 1). Gel A was stained with a polycarboxylate stain (alcian blue), while Gel B was stained for protein with Coomassie blue G-250 for 1 h. The humic bands in Gel B retained their original brown color while those in Gel A turned blue after staining. However, with overnight staining in Coomassie blue G-250, the humic bands acquired slight blue color (data not shown).

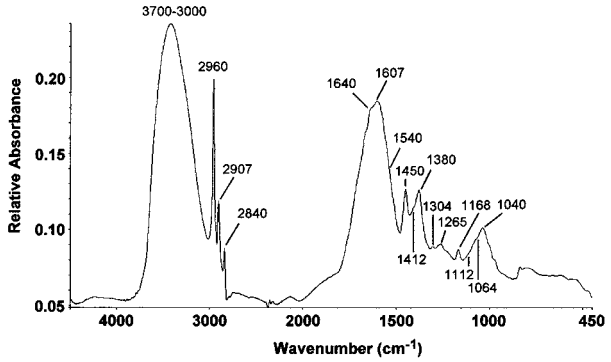

FIGURE 2. FT-IR spectrum of Tiron-treated Tinker HS FT-IR spectroscopy was performed as described in Materials and Methods. The labeled numerals are the wavenumbers (cm^{-1}) of spectral features that are discussed in the text.

FT-IR Spectroscopy. Tinker HS was dissolved in H_2O at 3 mg solid/mL, of which 50 μL was spotted onto a 4 μm thick Ultralene membrane and dried overnight at 40 °C under vacuum. This approach eliminated the reported reactions of humic substances with window salts, such as KBr, that has been used for transmission pellet or diffuse-reflectance measurements (*22*). Spectra were recorded on a Perkin-Elmer 1620 FTIR spectrometer with $LiTaO_3$ detector (Perkin-Elmer, Norwalk, CT), operating in transmission mode with bidirectional scan, moving mirror velocity of 0.3 cm/s, J-stop resolution of 4 cm^{-1}, acquiring a double-sided interferogram of 256 scans at 4 cm^{-1} resolution from 4500 to 450 cm^{-1}, which was Fourier transformed using the "strong" apodization setting. Raw spectra were subtracted against a blank membrane spectrum with a weighting factor of 1.0 to yield sample spectra. Background subtraction artifacts were small as evidenced by the region around 2370 cm^{-1}, where large contributions from the membrane have been well-canceled (see Figure 2).

Pyrolysis GCMS. Freeze-dried Tinker HS was weighed into quartz pyrolysis tubes and fixed into position using silanized quartz wool. The instrument and run conditions were similar to that previously described for HS (*13, 16*) and soils (*16, 23*), but a full description is given below due to numerous minor differences. The analytical pyrolysis system was a Pyroprobe 2000/AS2500 (CDS Inc., Oxford, PA), modified with a heated transfer line, interfaced to a Hewlett-Packard (Palo Alto, CA) model 5890 GC/5971A mass spectrometer system outfitted with a nonpolar column (0.15 mm i.d. × 50 m, 0.4 μm coat of BPX-5 5% phenyl-methyl silphenylene siloxane copolymer, SGE Inc., Austin, TX). The quartz sample tube was dropped under gravity into the pyrolysis chamber which was pneumatically off-line from the GCMS, followed by a 3-s delay to purge out residual air with a He flow of 20 mL/min, then the pyrolysis carrier gas path was switched to be on-line with the GCMS with a 0.3 s delay to stabilize pressure, the pyrolysis probe was heated at 1 °C/ms to 650 °C for 10 s, and volatile thermolyzates were swept by a He stream into the GC for 1 min, after which the pyrolysis system was switched back to off-line for thermal cleaning at 20 mL/min He flow for the duration of the analysis. The remainder of the analysis was conventional, with the thermolyzates eluting sequentially into the MS for detection. The pyrolysis injector block temperature was fixed at 280 °C, pyrolysis-injector transfer line was at 280 °C, the GC injector was at 280 °C, He carrier gas velocity was kept constant at 20 cm/s, injector split was 1:20, the column was temperature-programmed from 40 °C with 4 min hold to 290 °C at 10 °C/min, and the MS interface temperature was set to 300 °C. The mass spectrometer conditions were as follows: electron ionization mode, 70 eV electron energy, source/manifold temperature at 180 °C, electron multiplier voltage was 1458 V, acquisition from m/z 40−400, eight spectra averaged into one to yield 1.2 spectra/s, centroid processing of data to yield the mass histograms, and the system was calibrated to perfluorotributylamine using the "Autotune" function of the software.

Acid Digestion and Amino Acid Analysis of Tiron-Treated HS. Two to 3 mg of Tiron-treated HS powder was digested in sealed 2 mL glass vials under He in 0.2 mL of 6 N HCl (trace metal grade, Fisher Scientific) in the presence of 10 mM phenol and 1.25% (v/v) thioacetic acid at 110 °C for 12−36 h. A similar treatment of HS in doubly deionized water plus phenol and thioacetic acid at 110 °C was also performed as a control. Rigorous He purging was employed throughout to prevent oxidation of amino acids liberated from HS, while phenol and thioacetic acid were added to minimize the degradation of aromatic amino acids and methionine, respectively, during digestion. With this digestion procedure hydrolysis of amido amino acids (glutamine and asparagine) and degradation of cysteine was expected (*24*) and was observed. The digestion time course was compared for optimal recoveries for each amino acid, which was determined to be 19−24 h. At the end of digestion, the mixture was lyophilized to remove HCl, redissolved in doubly deionized water, centrifuged to remove insoluble materials, lyophilized again, and silylated in a 1:1 (v/v) mixture of acetonitrile and *N*-methyl-*N*-[*tert*-butyldimethylsilyl]trifluoroacetamide (MTBSTFA, Regis Technologies, Morton Grove, IL) for 3 h under sonication. The resulting *tert*-butyldimethylsilyl (*t*-BDMS) derivatives were directly analyzed by GCMS as described previously (*25*). For ^1H NMR analysis, a separate acid digestion was conducted on Tiron-treated HS (about 6−10 mg in 0.3−0.4 mL 1 or 6 N HCl) in the presence of thioacetic acid. The digests were similarly processed as described above, except that the MTBSTFA derivatization was omitted, and passage through the Chelex-100 (BioRad) resin was included to remove paramagnetic ions (*26*).

NMR Spectroscopy. Tinker HS was solubilized in D_2O or H_2O at 28 mg solid/mL in 5 mm NMR tubes (for ^1H spectra), 74 mg/mL in 8 mm tubes (for ^1H-^{13}C HSQC), or 46 mg/mL in 10 mm tubes (for one-dimensional ^{13}C and ^{31}P NMR spectra). At these concentrations, HS solutions remained clear throughout the measurement, but components may not be truly dissolved due to molecular aggregation which is expected from such colloidal material.

One-dimensional (1-D) ^1H NMR spectrum in D_2O was obtained at 11.75 T and 25 °C using a one-pulse sequence

with solvent-saturation, spectral width of 7 kHz, 90° pulse width, acquisition time of 1.17 s, interpulse delay of 2 s, and 128 transients, while that in H_2O was acquired at 14.1 T and 10 °C using a Watergate sequence (*27*) with similar parameters except for an an interpulse delay of 1.5 s and 64 transients. Directly detected 1-D ^{13}C and ^{31}P NMR spectra were recorded at 9.4 T on a Bruker AM400 spectrometer in D_2O using a 10 mm probe, with a 90° observe pulse and composite proton decoupling pulse (WALTZ-16 (*28*)) at 298 K. For ^{13}C NMR, the acquisition time of 0.508 s, recycle time of 1.19 s, spectral width of 23 809 Hz, and 122 880 transients were used. For the ^{31}P NMR spectra, the acquisition time was 1.376 s with a recycle time of 1.66 s, spectral width of 8065 Hz, and 49 697 transients. The 1-D data were processed using an exponential function with 3 Hz line-broadening. The spin−spin relaxation times (T_2) were estimated from the $T_{1\rho}$ experiment using a continuous wave spin-lock of 6.2 kHz B_1 field strength, as previously described (*13*) and 16 nonlinearly spaced spin-lock durations. Peak intensities were fitted to a double exponential decay function with an r^2 of >0.993, because fitting as a single exponential gave a very poor fit.

Phase-sensitive 2-D spectra were obtained on Varian Unity Plus instruments using the method of States et al. (*29*). Total correlation spectroscopy (TOCSY) spectra in D_2O were recorded at 14.1 T and 25 °C using MLEV-17 (*30*) for isotropic mixing for 37 ms at a B_1 field strength of 8.77 kHz, spectral width of 7000 Hz, interpulse delay of 1.5 s, acquisition time in t_2 and t_1 of 0.293 and 0.0357 s, respectively, and 48 transients per increment. NOESY spectra in D_2O were recorded at 14.1 T and 25 °C with a spectral width of 7000 Hz, mixing time of 200 ms, interpulse delay of 1.5 s, acquisition times in t_2 and t_1 of 0.293 and 0.0274 s, respectively, and 40 transients per increment. NOESY spectra in H_2O were recorded similarly except at 10 °C using the Watergate method (*27*) for solvent suppression and 96 transients per increment. ^1H-^{13}C-HSQC spectra (*31*) were recorded at 11.75 T and 25 °C using pulsed field gradients for coherence selection and elimination of unwanted magnetization (*11*), spectral width of 5000 Hz, interpulse delay of 1.3 s, acquisition time in t_2 and t_1 of 0.102 and 0.011 s, respectively, and 512 increments with 208 transients per increment. For all 2-D processing, the data in both dimensions were weighted by an exponential (2 Hz line broadening) and mild Gaussian functions, while those in t_1 were also linear predicted to twice the data length, before zero-filling to 8k × 2k and Fourier transformation. ^1H NMR spectra were referenced to HOD at 4.76 ppm, while ^{13}C NMR spectra were referenced indirectly from the proton shifts according to the gyromagnetic ratio (*32*). ^{31}P NMR spectra were referenced to external methylene diphosphonate at 0 ppm (*33*).

Two-dimensional ^1H TOCSY of the acid digest of Tinker HS was acquired at 14.1 T at 25 °C with a spectral width of 6000 Hz, interpulse delay of 2 s, B_1 field strength of 8.35 kHz, isotropic mixing time of 46.2 ms, acquisition time in t_2 and t_1 of 0.341 and 0.0583 s, respectively, and 16 transients per increment. 2-D Fourier transformation with a Gaussian weighting in both dimensions was performed to give a 8k × 2k data matrix.

Results

Elemental Profile of Tiron-Treated Tinker HS. The elemental profile of Tinker HS, as determined by C/N analyses and ED-XRF, is shown in Table 1. Carbon was the most abundant element measured, followed by N, Al, K, P, S, Fe, Ca, and other metals. Na, Cl, and Si were also present, but they were not quantified (data not shown), and some common soil mineral elements such as Ti were below detectable limits. The natural abundance isotope ratio for ^{13}C ($\delta(^{13}C)$) and ^{15}N ($\delta(^{15}N)$) of the Tinker HS were −24.77 and 2.10, respectively. The value for $\delta(^{13}C)$ is referenced to the same scale as the isotope ratio reference material NIST 8563 CO_2 of petrochemical origin (−41.56), while $\delta(^{15}N)$ is scaled to air as zero, as is the convention. The $\delta(^{13}C)$ value is between those of fossil materials and inorganic carbonate (−23.83) and is consistent with an origin from the pine (C3 plant) forest. Table 1 shows a persistent inorganic composition for the Tinker HS, not removed by the Tiron treatment. This result is consistent with the ash content of 21% for Tiron-treated HS. While ashing is commonly employed for the estimation of inorganic content, the choice of method—and therefore the results—is somewhat dependent on the inorganic structures present. Too low an ashing temperature can result in incomplete combustion of the organic portion, while too high a temperature can result in loss of structural water from mineral fragments (*34*) that may be present in HS preparations. In this study, the Tinker HS samples were ashed at 550 °C, which was considered to be the most appropriate, since for the parent soil, this temperature was high enough to give inorganic content in accordance with the C/N (oxidizable carbon) analysis, while cool enough to minimize loss of mineral bands as determined by FTIR (*16*). It is also interesting to note that the ash content of HS before Tiron treatment (48%) was substantially higher than that (21%) of Tiron-treated HS, indicating the efficiency of metal ion removal by the treatment. The remaining transition metals and Al may be tightly (e.g. covalently) associated with the HS in mineral forms (*35*) and/or inaccessible to Tiron.

Characterization of Tiron-Treated Tinker HS by SDS-PAGE, FT-IR, and Pyrolysis-GCMS. The Tiron-treated Tinker HS was characterized by these methods to aid the interpretation of NMR analysis below.

SDS-PAGE. The electrophoretic pattern of Tinker HS (lanes 3 and 4) is shown in Figure 1A (stained with alcian blue) and 1B (stained with Coomassie blue G-250), along with that of IHSS soil humic standard (lane 2). Both HS exhibited a similar pattern of three sharp brown bands, two fast (*b* and *c*) and one slow moving (*a*) relative to the peptide standards (3.5−25.6 kD) in lane 1 (Figure 1B). The different electrophoretic mobility of these bands may be related to their difference in charge density and/or sizes with $c > b > a$. The similar band pattern of Tinker and IHSS HS was interesting and suggests some commonality in their structure components. These bands reacted with alcian blue which stains polycarboxylate (*21*) but very weakly with Coomassie blue G-250 which stains proteins and peptides. The affinity of these HS for alcian blue (Figure 1A) revealed their polycarboxylate nature, consistent with the FT-IR analysis described below. The weak interaction of either HS with Coomassie blue G-250 suggests that they did not contain a large amount of noncovalently bound proteins. However, this result did not rule out the presence of a small amount of covalently linked peptides in these HS. In fact, the combination of NMR, FT-IR, and py-GCMS analyses (see results below) affirmed the occurrence of peptide segments in Tinker HS.

FT-IR. Figure 2 shows the FT-IR spectrum of Tiron-treated Tinker HS. The band assignment below is biased toward those functional groups considered to occur in humic substances e.g. refs *16* and *36*, and the discussion below is limited to bands concerning confirmation of the NMR results. The bands at 2960 and 2907 cm^{-1} could represent C−H asymmetric and symmetric stretch of CH_2, e.g. aliphatic groups. Whole Tinker soil prominently exhibited the same bands (*16*). The aliphatic assignment is supported by the resolved band at 1450 cm^{-1}, which is diagnostic of aliphatic C−H bend and deformation of CH_3. For aliphatics, the size of this band is as expected, relative to the C−H bands at 2960 and 2907 cm^{-1}.

At 1607 cm^{-1} is the carboxylate C═O asymmetric stretch of ionized carboxylates, consistent with the alcian blue

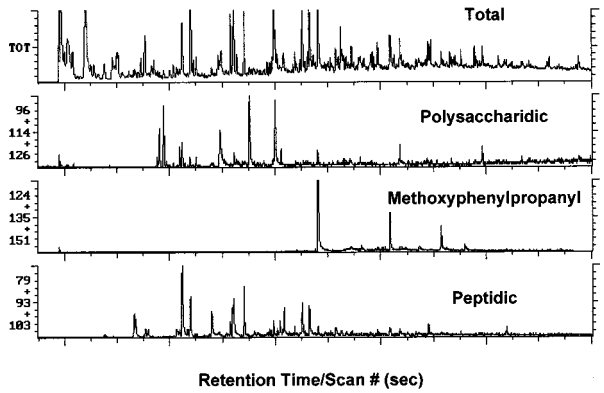

FIGURE 3. Pyrolysis-GCMS chromatograms of Tiron-treated Tinker HS Pyrolysis-GCMS was performed as described in Materials and Methods. As discussed in the text, the method of data presentation here is according to Faix et al. (*38*), with each panel showing the total ion tracing (TOT) together with the summed selected ion chromatograms of *m/z* 96+114+126 for "polysaccharidic", *m/z* 124+135+151 for "methoxyphenylpropanyl", and *m/z* 79+93+103 for "peptidic" markers. This figure is meant to be only illustrative. The presence of these structures were supported by a much more comprehensive reduction of the py-GCMS data (data not shown), as described in the text.

staining in SDS-PAGE. The broadness of this peak system suggests considerable heterogeneity of carboxylate structures, partially masking the peptide "amide II" N−H bending (at 1540 cm^{-1} for bovine serum albumin). The second derivative of the spectrum (data not shown) confirmed the presence of a peak at 1540 cm^{-1} in Tinker HS. The shoulder at ≈1640 cm^{-1} is typical of peptidic C═O stretch (amide I). Taken together, the amide II and peptidic C═O bands indicate that the peptides are relatively minor components. The prominent band at 1380 cm^{-1}, with a shoulder at 1412 cm^{-1}, can be attributed to either aliphatic C−H bend or carboxylate C═O symmetric stretch. Support for lignin-type residues comes from bands at 1304 and 1265 cm^{-1} which are indicative of the C−OH stretch of phenolics, and at 2840 cm^{-1} is a band that can represent CH_3 bending overtone in methoxy groups.

At 3700−3000 cm^{-1} is the OH band; in humic substances, this region is usually attributed to cellulosic residues and phenolics, but it could also contain contribution from structural water in mineral fragments, as is the case with Tinker soil (*16*). The resolved band at 1168 cm^{-1} and peaks centered around 1040 cm^{-1} is indicative of residual cellulosic material, based on cellulose standards (data not shown and ref *16*). However, if only cellulose was present, there should also be bands at 1112 and 1064 cm^{-1} that are at least the size of the one at 1168 cm^{-1}. The fact that they are only slight shoulders or less suggests that this peak complex also represents the Si−O stretch of silicates, possibly including Al−OH stretch of aluminosilicates as observed in whole soil (*37*). This possibility is consistent with the large amount of Si and some Al found by ED-XRF analysis (Table 1). In the parent Tinker soil, this region coincided well with FT-IR spectra of the constituent silicate minerals (*16*).

Pyrolysis GCMS. Figure 3 shows three different selective ions plus the total ion tracings from the py-GCMS analysis of Tinker HS. Because metal ions can alter the pyrolytic pattern, e.g. ref *13*, and given the present uncertainty concerning the organic association with the persistent metals in Table 1, the method is used here primarily in a qualitative fashion. The method of representation in Figure 3 is from Faix et al. (*38*), illustrating a subset of markers for the presence of lignoid phenolics (e.g. methoxyphenylpropanyl), peptidic, and polysaccharidic structures. Numerous other markers for these structures, e.g. refs *16*, *23*, *39*, and *40*, were also present (data not shown) and agreed with py-GCMS analysis of the

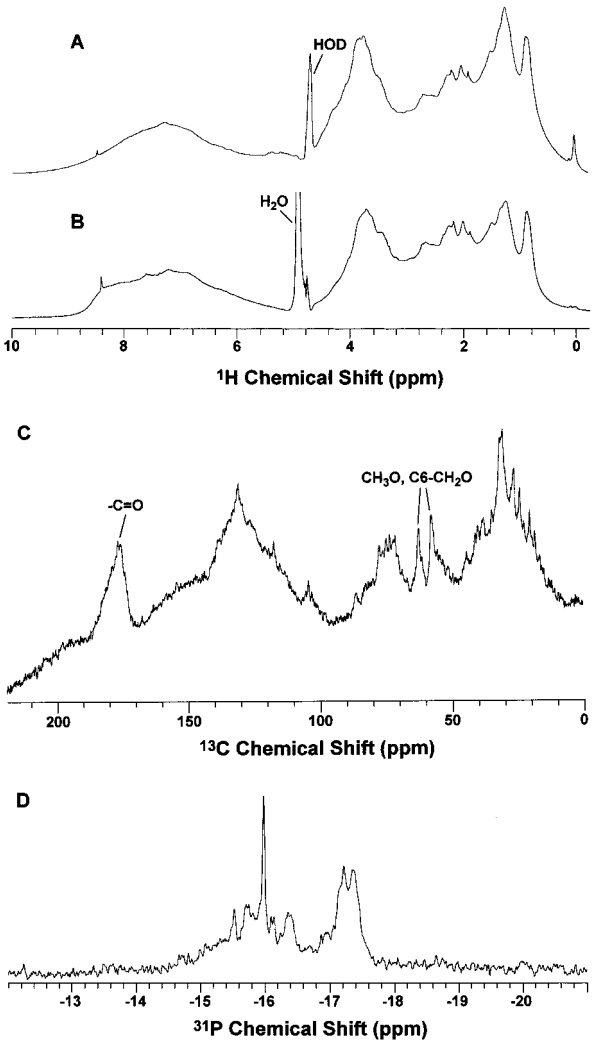

FIGURE 4. 1-D NMR spectra of Tiron-treated Tinker HS. The ^{1}H NMR spectrum in D_2O (A) was obtained at 11.75 T and 25 °C, while spectrum in H_2O (B) was acquired at 14.1 T and 10 °C using a Watergate sequence (*27*), both as described in Materials and Methods. The ^{13}C NMR (C) and ^{31}P NMR spectra (D) were acquired in D_2O at 9.4 T as described in Materials and Methods.

parent Tinker soil (*16*). The presence of these markers lent support to the NMR assignments described below.

NMR Spectroscopy. One-Dimensional (1-D) NMR. The 1-D ^{1}H, ^{13}C, and ^{31}P NMR spectra of the Tiron-treated Tinker HS are shown in Figure 4. These spectra were significantly better resolved in terms of peak overlap than those without the Tiron treatment (data not shown). Tiron treatment also eliminated the need for high pH to solubilize the HS. This is advantageous because high pH—which risks oxidation and hydrolysis—can be avoided so that experiments can be extended into normal soil pH ranges and long spectral acquisition times. The spectral improvements apparently resulted from the removal of exchangeable metal ions, as inferred from the reduction in ash content and the blue-green color of the Tiron wash, which is characteristic of Tiron chelates with Fe and Cu. These metal ions, particularly paramagnetic ones, could broaden NMR resonances via the effect of unpaired electrons and/or exchange with the anionic groups of the HS. Broadening could also be caused by the aggregating effect of metal ions on the HS possibly resulting from charge neutralization (*41*). In particular, the broadening effects should preferentially degrade signals of chelator groups such as the carboxylate and phosphate, possibly rendering them invisible to NMR. In the present case, the

distinct presence of the carbonyl and phosphate resonances in Figure 4C,D demonstrated the efficacy of the Tiron treatment for NMR spectroscopy. Another important advantage of the treatment was that Tiron did not bind to HS irreversibly and was easily removed by rinsing acid-precipitated HS with dilute HCl. This was not the case with the common chelators EDTA and EGTA, which remained prominent in NMR spectra of HS even after extensive dialysis (data not shown).

From the one-dimensional (1-D) spectra—coupled with information from SDS-PAGE staining, FT-IR, and py-GCMS analyses—an initial assessment of chemical groups present in the Tinker HS could be obtained. The ^{1}H spectra (Figure 4A,B) show a broad envelope for the aromatic groups centered at ca. 7.5 ppm, weak signals near 4.6−5.5 ppm which are characteristic of α-anomeric protons in pyranoses, and partially resolved resonances in the methine (ca. 3.2−4.6 ppm), methylene (1.5−4 ppm), and methyl (0−3.5 ppm) regions (*42*). The 1-D ^{1}H spectrum in H_2O (Figure 4B) shows additional intensity near 8−8.5 ppm as compared to the spectrum in D_2O (Figure 4A). These signals arose from exchangeable protons, such as those from unstructured peptide NH (*10*), which were not observable in D_2O (Figure 4A) due to exchange of H by D. Free amino groups also occur in this shift range, but their contribution is expected to be minor due to their much faster exchange rates at the pH (6.0) of the HS preparation.

The 1-D ^{13}C spectrum (Figure 4C) exhibited two categories of resonances: one with very broad appearances and the other of more discernible peak shapes that rose above the broad components. The chemical shifts of the discernible components support the presence of such chemical groups as the carbonyls at ca. 170−180 ppm (e.g. those from carboxylates, amides, and peptides), aromatic heterocycles at 140−160 ppm (e.g. pyridines, pyrimidines, and purines), aromatics at 120−140 ppm (e.g. phenolics), possible sugar anomerics at 90−110 ppm, aliphatic methine, and methoxy (60−80) (e.g. α-amino acids and alcohols), methylene (30−50 ppm), and alkyl methyl groups (20−30 ppm). These resonances arose presumably from the more mobile and smaller sized components of the HS preparation. The broad resonances that may have contributed to the sloping baseline in Figure 4C could be attributed to the more rigid and larger molecular aggregates (e.g. ≥30 nm size particles as evident from NMR diffusion measurement, data not shown). Such a dependence of resonance intensity on molecular sizes makes it impractical to estimate total functional groups in a humic preparation.

Figure 4D illustrates the ^{31}P NMR spectrum of Tinker HS at pH 5.7 where distinct and partially resolved resonances between −15.5 and −17.5 ppm along with a weak resonance near −20 ppm were observed. This shift range (referenced to methylene diphosphonate) is typical of phosphodiesters as found in phospholipid metabolites including glycerophosphoryl ethanolamine (GPE) and glycerophosphoryl choline (GPC), polyphosphates, and nucleic acids (*32, 42*). The presence of appreciable amounts of P in HS (2.10%, Table 1) supports the observed strong ^{31}P NMR signal, while their relatively sharp appearance may be related to a mobile nature of the respective phosphorylated side chains.

The chemical group information obtained from the preceding 1-D NMR spectra was based on chemical shifts alone, which can lead to erroneous assignments because different chemical groups have overlapping chemical shift ranges (*42*). For example, methoxy groups, implicated by FT-IR analysis, have chemical shifts in the methine group range (e.g. 3.5−4.0 ppm). It is therefore necessary to obtain additional NMR parameters to help resolve the ambiguity. In addition, the combination of broad and overlapping resonances greatly limits the number of chemical groups

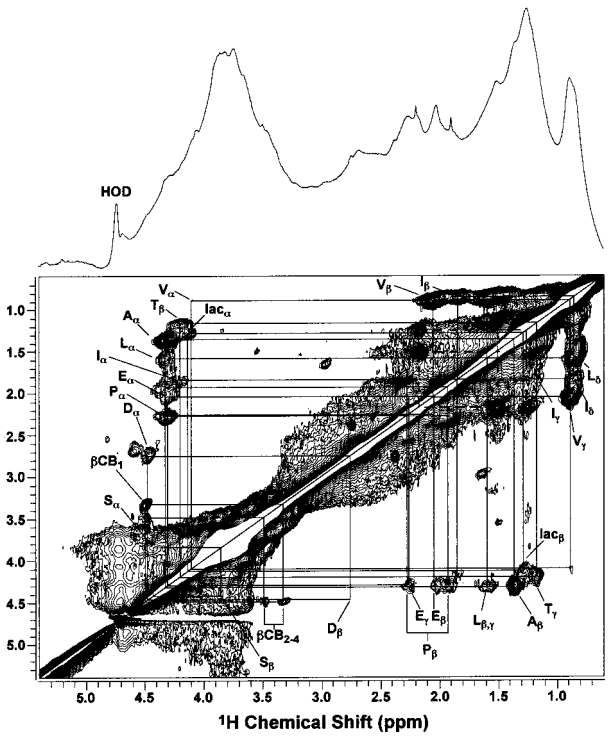

FIGURE 5. 2-D ^{1}H TOCSY spectrum of Tinker HS in D_2O. The TOCSY spectrum was acquired at 14.1 T as described in Materials and Methods. The 2-D spectrum is displayed as contour plot along with the 1-D high-resolution spectrum. The peptidic amino acid resonances were assigned based on scalar coupling patterns and tabulated chemical shifts (*44*). I, isoleucine; L, leucine; V, valine; T, threonine; A, alanine; E, glutamate; P, proline; D, aspartate; *β*CB, *β*-cellobiose-like carbohydrate.

that can be distinguished from 1-D NMR spectra of HS. Therefore, we have conducted several 2-D NMR experiments on the Tinker HS to improve the spectral resolution and to deduce structures and dynamics of extended molecular fragments based on the patterns of scalar coupling and dipolar interactions. It should also be noted that solution-state NMR (particularly TOCSY and HSQC experiments) preferentially detects mobile rather than rigid parts of the structure such that mobile groups can dominate the spectrum even though they may be relatively minor components.

Two-Dimensional (2-D) Homonuclear NMR. Figure 5 shows the ^{1}H TOCSY spectrum of the Tinker HS in D_2O, where quite a few off-diagonal cross-peaks are evident (traced by rectangular boxes). These cross-peaks indicated the intramolecular scalar coupling (covalent bonding) between pairs of protons. It is also notable that the cross-peaks were relayed less extensively (≤3 bonds) in this spectrum than is typically observed in the spectra of small molecules that have long ^{1}H T_2 values (i.e. sharp resonances). This was a consequence of the comparatively short T_2 values (estimated from the $T_{1\rho}$ expeiment to be 20−30 ms for the sharpest HS resonances), which limited the length of the isotropic mixing time (37 ms) that could be used. These T_2 values are consistent with the macromolecular nature of the HS. In addition, the $T_{1\rho}$ experiment revealed a second very rapidly decaying component with T_2 of <5 ms, which accounted for >40% of the total intensity and presumably arose from very large molecular aggregates (*43*). This component would not yield significant cross-peaks in TOCSY experiments.

The intense cross-peaks connecting methyl groups near 0.9 ppm to peaks near 1.6−2.1 ppm and then to peaks near 4.1−4.3 ppm were characteristic of substituted propyl and isopropyl groups bearing an electronegative group at the

methine carbon, such as in the amino acid residues valine, leucine, and isoleucine in peptides (*44*). Other strong cross-peaks between the methine region and the methyl region (4.3−1.37 and 4.3−1.18) indicated the presence of the substructure X,Y−CH−CH_3 where X and Y were electronegative groups. These chemical shifts are similar to those of alanine and threonine residues when followed by alanine in random-coil peptides. By tracing the cross-peak patterns in this way, we found that many of the intense cross-peaks in the TOCSY spectrum corresponded to aliphatic amino acid side chains in peptides, particularly as residues followed by alanine (*44*). Moreover, the clear observation of these cross-peaks indicates that these side chains are relatively mobile (see also below).

Another group of intense cross-peaks at 1.25, 1.5, and 2.2 ppm (traced by dashed rectangular boxes) could be derived from $-CH_2(CH_2)_nCH_2COOR$ type of aliphatic structures such as those from plant cuticle residues, possibly abundant in forest derived HS (see also Figure 7 for HSQC data). This is also supported by the FT-IR observation of a considerable abundance of aliphatics (Figure 2) as discussed earlier, plus the abundance of m/z 55 and m/z 57 ions from py-GCMS (data not shown). However, it would be difficult to confirm this NMR assignment without additional evidence due to the lack of sufficiently resolved TOCSY pattern for the extended CH_2 chains in cuticle-like structures. The cross-peaks from 3.3 to 4.1 to 4.5−4.7 ppm and in the aromatic region between 6.8 and 7.1 ppm (data not shown) were less intense and may arise from carbohydrate- and phenolic-like structures, respectively. For example, the cross-peaks at 3.32, 3.5, and 4.49 ppm were characteristic of the nonreducing glucose residue of a β-cellobiose-like structure (*42*), while those at 6.8 and 7.1 ppm (data not shown) were consistent with a peptidic tyrosine residue (*44*). These weak cross-peaks may result from a small coupling between the pairs of interacting protons.

The above TOCSY analysis was supported by the result obtained from the NOESY experiment where dipolar interactions, between pairs of protons that were in spatial proximity, were revealed as off-diagonal cross-peaks. The ^{1}H NOESY spectra of Tinker HS were recorded in both D_2O (Figure 6A) and H_2O (Figure 6B), which displayed some similar cross-peaks in the 1−4 ppm region to those in the TOCSY spectrum (Figure 5). These cross-peaks arose from through-space interactions between protons of amino acid side chains because these scalar coupled protons are also close in space. However, the cross-peak intensities in the TOCSY and NOESY spectra were not comparable; the more intense peaks in the TOCSY were much weaker in the NOESY spectra and vice versa. This implies a considerable mobility of the amino acid side chains and their direct exposure to solvent (*45*). It should also be noted that all of the cross-peaks in the NOESY spectrum had the same sign (negative) as the diagonal peaks, which established their origin from macromolecules and is consistent with the peptide (instead of free amino acid) assignment.

In addition to the TOCSY-type cross-peaks in Figure 5, there were NOESY cross-peaks for which no corresponding TOCSY cross-peaks were evident (Figure 6 and data not shown). These included the cross-peak between the group of resonances at 8−8.5 ppm and 4−4.4 ppm as well as those connecting 7−7.3 ppm to 3.8−3.9 ppm, to 2.0 ppm, and then to 0.9 ppm (Figure 6B). As evident from the 1-D ^{1}H data shown above (cf. Figure 4), the 8−8.5 resonance could be the NH of unstructured peptides. This assignment is now supported by the NOESY (Figure 6B) cross-peaks from 8 to 8.5 ppm to 4−4.4 ppm, which is highly characteristic of the dipolar interaction between NH and CHα of amino acid residues in random coil peptides. This assignment is further substantiated by the *lack* of such interaction in the NOESY

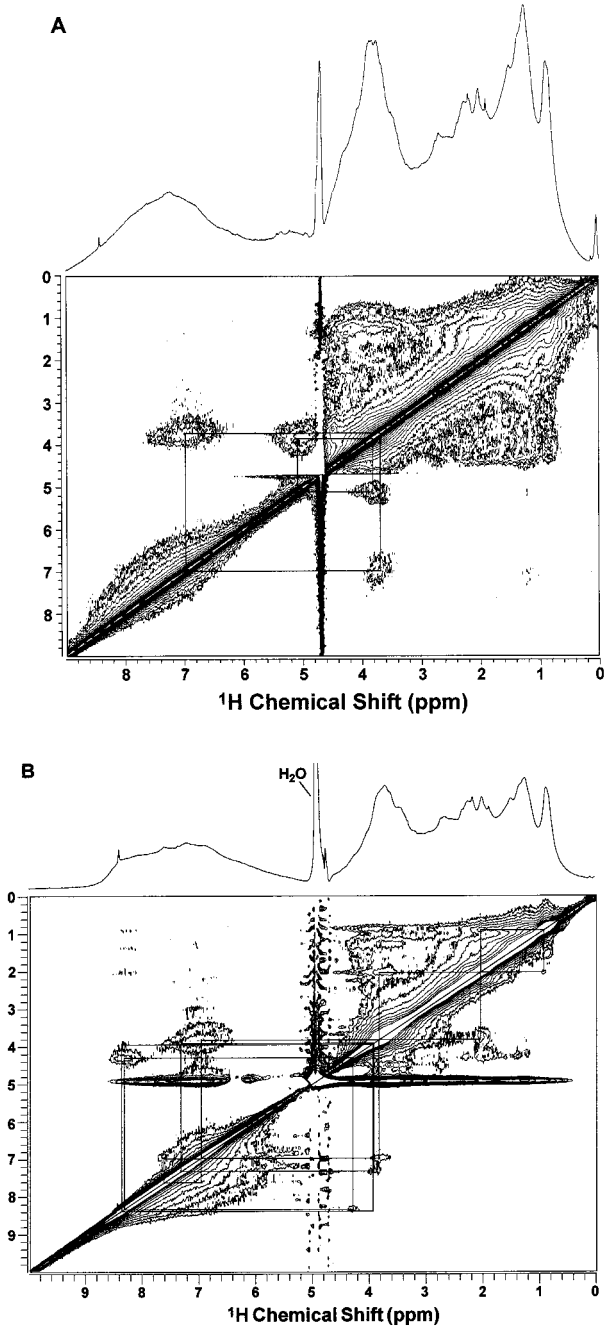

FIGURE 6. 2-D ^{1}H NOESY spectrum of Tinker HS in D_2O and H_2O. The NOESY spectra in D_2O (A) and in H_2O (B) were recorded at 14.1 T as described in Materials and Methods. The two spectra are displayed as contour plots along with the high-resolution 1-D spectrum.

spectrum acquired in D_2O (Figure 6A), confirming the participation of the exchangeable NH in this dipolar interaction. This result also excluded the possibility of other structures (e.g. $RCOOCH_2$- or Aryl-OCH_2-) that may contain methylene protons contributing to the 4−4.4 ppm region. The relayed NOESY connectivity from 7 to 7.3 to 0.9 ppm pointed toward a methoxyphenyl propanyl type of structure (of possible lignin origin), with peaks at 7−7.3, 3.8−3.9, 2.0, and 0.9 ppm assigned to phenyl, methoxy, and propanyl protons, respectively (see also HSQC data in Figure 7). This assignment is consistent with the lack of scalar connectivity from 7 to 7.3 to 3.8−3.9 ppm and the abundance of such structure in Tinker HS, implicated by FTIR (Figure 2) and py-GCMS analysis (Figure 3). However, the expected TOCSY

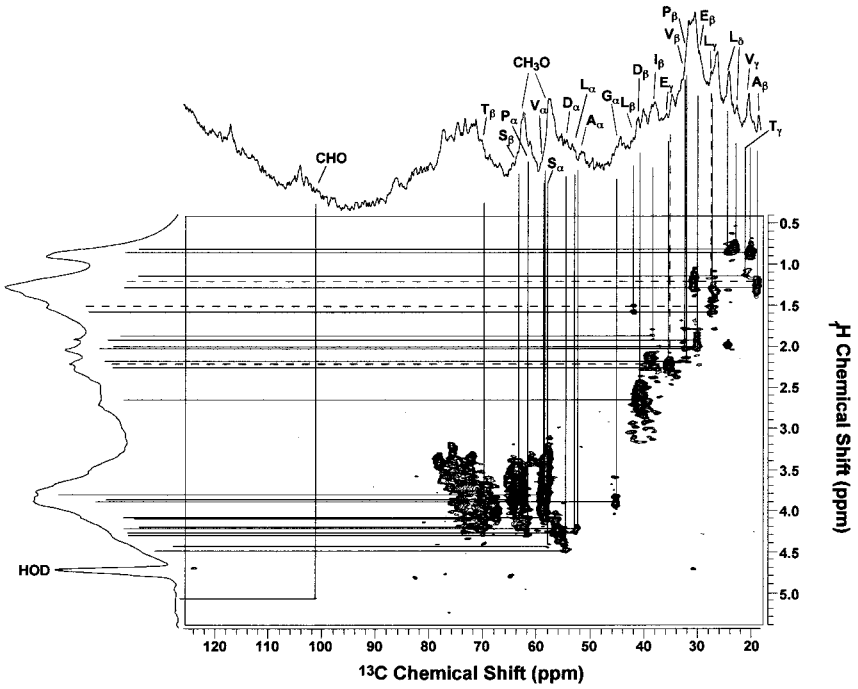

FIGURE 7. ^{1}H-^{13}C HSQC spectrum of Tinker HS in D_2O. The HSQC spectrum was acquired at 11.75 T and 25 °C as described in Materials and Methods. The spectrum is displayed as contour plot along with the high-resolution 1-D ^{1}H and ^{13}C spectra.

cross-peak between the 2.0 and 0.9 ppm protons was missing (cf. Figure 5). This missing interaction could be a consequence of a rigid environment, short T_2, and/or weak coupling.

A third type of NOESY cross-peaks included those connecting a group of resonances at 5−5.4 ppm to those at 3.6−4.2 ppm (Figure 6A). The corresponding scalar connectivities were visible but weaker in the TOCSY spectrum (Figure 5). The resonances in the 5−5.3 ppm range were recently assigned to olefinic protons (*12*), but the observed 2-D cross-peak patterns for Tinker HS are not consistent with this assignment. Instead, they were typical of dipolar and scalar interactions between the anomeric and other ring protons of α-pyranose-containing carbohydrates (*42*). This assignment was also consistent with the 1-D ^{13}C NMR spectrum (Figure 4C) and 2-D HSQC spectrum (Figure 7) described below. It further agreed with the presence of sugar resonances in the 1 N HCl digest of Tinker HS (see below), FT-IR (1168 cm^{-1} band, Figure 2), and py-GCMS data (Figure 3). It should be noted that the occurrence of sugars in many humic digests has been implicated previously (*4*). However, it remained to be ascertained whether the carbohydrate moiety was covalently linked to other structure components of the colloidal HS.

2-D Heteronuclear NMR. To gain further evidence for the above 1-D and 2-D homonuclear assignments, a 2-D ^{1}H-^{13}C HSQC spectrum of the Tinker HS was acquired to reveal the coupling between ^{13}C and its directly bonded proton(s) as cross-peaks. As shown in Figure 7, the high field proton resonances near 0.9 ppm were connected to the high field carbon resonance near 20 ppm, which are characteristic of the methyl groups from alanine, valine, and leucine (*42*). In addition, many of the methine resonances (52−64 ppm) had ^{13}C chemical shifts (*44*) in accord with the amino acids assigned from the ^{1}H TOCSY (Figure 5) and NOESY spectra (Figure 6). For those ^{1}H resonances at 1.25, 1.5, and 2.2 ppm (Figure 5), the coupled ^{13}C resonances appeared be 19, 28, and 35 ppm, respectively (dashed line, Figure 7), which supports their origin from long alkane chains (*42*) such as those in plant cuticles.

Also seen in Figure 7, two relatively distinct ^{13}C resonances near 59 and 64 ppm were connected to a group of ^{1}H resonances around 3.3−4.1 ppm. These shifts are consistent with methoxy groups and the C6 methylene protons of hexoses. Both types of structures were implicated by the FT-IR (Figure 2) and py-GCMS (Figure 3) analyses, appeared to be present in whole Tinker soil (*16*), and have often been reported to be present in natural organic matter (*46, 47*). In addition, the general lack of TOCSY connectivity from the 3.3−4.1 ppm region to other regions in Figure 5 is consistent with the assignment of methoxy and/or hexose C6 protons since these protons should display none or weak coupling to adjacent protons, respectively. Moreover, the coupling of carbon at 59 ppm to protons in the 3.8−3.9 ppm region is compatible with the assignment of methoxyphenyl propanyl structures deduced from the NOESY data (Figure 6B). Thus, the HSQC (Figure 7), TOCSY (Figure 5), NOESY (Figure 6), FT-IR (Figure 2), and py-GCMS (Figure 3) data combined lent stronger support for these assignments.

It is also interesting to note that, although the ^{13}C chemical shifts of the methoxy and/or hexose C6 groups were relatively distinct, the corresponding ^{1}H shifts appeared to be more dispersed (Figure 7). Upon closer examination, the chemical shift dispersion was ca. 4 and 0.9 ppm for the ^{13}C and ^{1}H resonances, respectively, which amounted to ca. 450 Hz spread in both cases. This phenomenon was unexpected and difficult to explain. It could arise from the "amorphous" and "colloidal" (dispersive) nature of humic substances. For example, some of the methoxy groups could be in various orientations to aromatic rings as in methoxyphenyl propanes, whose ring currents produce local magnetic fields that can cause a similar dispersion on chemical shift (measured in Hz) for both ^{1}H and ^{13}C (*48*).

The strong cross-peaks between 70 and 80 ppm (^{13}C) and 3.5−4 ppm (^{1}H) in Figure 7 were unlikely to have originated from amino acids but are consistent with those of carbohydrates (*42*). This also agreed with the presence of anomeric protons in the 5−5.4 ppm range (Figures 4−6). However, except for a weak cross-peak near 102 ppm (^{13}C) and 5.1 ppm (^{1}H), the representative anomeric region of 94−105 (^{13}C) and 4.5−5.4 (^{1}H) ppm was devoid of cross-peaks (Figure 7). This could indicate a small coupling between the anomeric carbon and protons in the Tinker HS. The TOCSY and HSQC

TABLE 2. Amino Acid Composition of the Acid Digest of Tinker HS[a]

components[b]	Tinker HS (μmol g^{-1}) (dry wt) 6 N HCl	H_2O	components[b]	Tinker HS (μmol g^{-1}) (dry wt) 6 N HCl	H_2O
lactate	8.72	0.23	Thr	64.74	0.1
Ala	41.82	0.83	malate	1.9	1.6
Gly	52.51	0.4	Phe	10.58	0.08
Val	26.96	0.19	Asp+Asn	31.05	1.68
Leu	29.91	0.2	OH−Pro	6.41	0.16
Ile	15.05	0.11	Cys	2.74	ND
succinate	3.42	2.93	Glu+Gln	24.47	ND
GAB	0.13	0.12	Lys	0.84	ND
Pro	14.09	0.53	His	ND	ND
fumarate	1.57	3.98	Tyr	1.69	ND
phosphate-containing	4.59	2.02			
Ser	21.83	0.1	total mg AA/g HS	40.13	0.51
Met	1.71	0.03	% (w/w) N from AA	0.5	

[a] Tiron-treated HS was hydrolyzed and analyzed by GCMS as described in the Materials and Methods. The digestion conditions were 110 °C in 6 N HCl or in H_2O for 12−19 h. Ala, alanine; Gly, glycine; Val, valine; Leu, leucine; Ile, isoleucine; GAB, γ-aminobutyrate; Pro, proline; Ser, serine; Met, methionine; Thr, threonine; Phe, phenylalanine; Asp, aspartate; Asn, asparagine; OH−Pro, hydroxyproline; Glu, glutamate; Gln, glutamine; Lys, lysine; His, histidine; Tyr, tyrosine. [b] μmol/g HS dry wt for all components.

experiments detected only those protons or carbons for which the effective T_2 value was larger than or comparable to the reciprocal of the coupling constant (ca. $^3J_{HH} \sim 7$ Hz for aliphatic and alkyl groups, $^1J_{CH} \sim 150$ Hz). The aromatic region of the HSQC spectrum also lacked cross-peaks (data not shown), which is similar to the case for the TOCSY spectrum (Figure 5 and data not shown). This presumably resulted from the rapid decay of signals during the HSQC preparation period owing to very short ^{13}C T_2 values (<3 ms) of the aromatic carbons, which may in turn be attributed to the macromolecular and immobile nature of these carbons (*12*) in Tinker HS.

Thus, the combination of 1-D and 2-D ^1H, ^{13}C, and ^{31}P NMR characterization of the Tinker HS preparation provided unprecedented details about its component structure, not practical to achieve by 1-D NMR analysis alone or other single methods. The confidence in these structure assignments was further corroborated by other independent analyses including SDS-PAGE, FT-IR, and py-GCMS. In addition to structure characterization, the 2-D solution-state NMR approach also provided clues on the relative mobility of various chemical moieties.

^1H NMR and GCMS Analysis of Acid Digests of Tinker HS. The above NMR analysis of the Tinker HS preparation indicated the abundance of resonances arising from relatively mobile peptidic amino acids and carbohydrates. To further confirm these assignments, Tinker HS was digested in 1 or 6 N HCl, and the digests were subjected to analysis by ^1H NMR as well as MTBSTFA silylation followed by GCMS analysis. Because digestion of any HS will produce numerous non-amino acid interferences, the structure-confirming NMR and GCMS methods for amino acid analysis were necessary. The 6 N HCl digest gave a comparable amino acid profile as the 1 N HCl digest, except for the degradation of sugars in the former. Therefore, 1 N HCl digestion may be more appropriate for the recovery of both amino acids and sugars from humic materials. The compounds present in the HCl digests were identified by comparing the ^1H chemical shifts and scalar coupling patterns obtained from the ^1H TOCSY spectrum of the 1 N HCl digest (Figure 8) with those of the standards (*42*). The corresponding sets of scalar coupling patterns as those traced for the peptidic amino acids in Figure 5 are displayed in Figure 8, except for tyrosine, phenylalanine, and glycine which gave no cross-peaks in this region in the intact HS. For glycine, this is to be expected since it has no scalar coupled protons in D_2O, while for tyrosine and phenylalanine, the lack of connectivity from β to α protons in the intact HS could result from a low concentration and/or short T_2 (e.g. lower mobility) (see above).

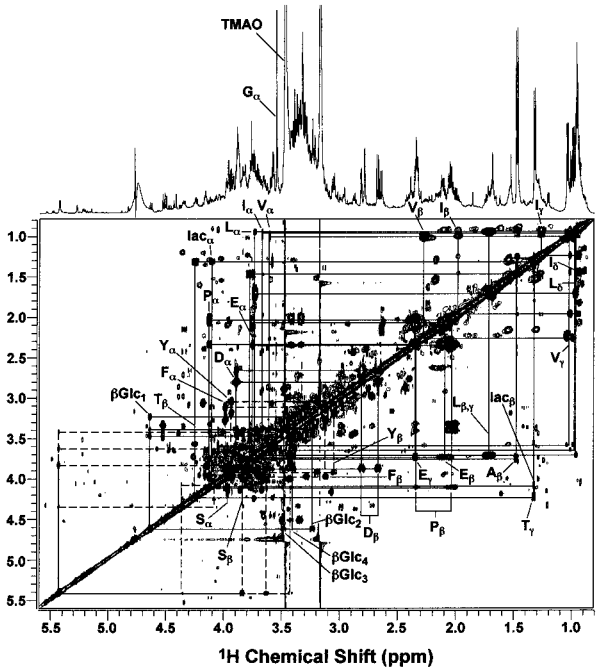

FIGURE 8. 2-D ^1H TOCSY spectrum of acid digest of Tinker HS. The HS was digested in 1 N HCl for 24 h and the TOCSY spectrum was acquired at 14.1 T as described in Materials and Methods. The spectrum is displayed as contour plot along with the high-resolution 1-D spectrum. The resonances were assigned based on scalar coupling patterns and chemical shifts compiled by Fan (*42*). Solid lines trace the corresponding coupling patterns as those in Figure 5 while dashed lines indicate those missing or not discernible in Figure 5. The letter designations are the same as those in Figure 5. In addition, lac denotes lactate, G, glycine, TMAO, trimethylamine-*N*-oxide, βGlc, β-glucose, Y, tyrosine, and F, phenylalanine.

It is notable that the chemical shifts of the free amino acids in the digest (Figure 8) deviated significantly from those in the intact Tinker HS (Figure 5), which reaffirmed the peptidic nature of these amino acids in intact HS. Thus, the NMR data of the digest verified the assignments of various peptidic amino acid residues present in the Tinker HS structure. In addition, several α- and β-sugars (including β-glucose) were evident in the TOCSY spectrum of the digest (Figure 8), which lent a strong support to the carbohydrate assignment for intact Tinker HS in Figures 5−7 (see above).

The amino acids in the digests were also confirmed and quantified by GCMS as shown for the 6 N HCl digest in

Table 2. The abundance of amino acids in the Tinker HS followed the order Thr ≈ Gly > Ala > Asp+Asn ≈ Val ≈ Leu ≳ Glu+Gln ≈ Ser > Ile ≈ Pro > Phe > OHPro > Tyr ≈ Met > Lys (Table 2). Except for threonine, this profile is similar to those observed for both terrestrial and stream humics (*4*). The high Thr, Gly, and Asp+Asn content in Tinker HS should contribute toward its water solubility. Interestingly, this amino acid profile is atypical of proteins in live organisms. Apart from those completely or partially degraded by the digestion process (Trp, Cys, cystine, Gln, and Asn), the residues His, Lys, Tyr, and Met were underrepresented, while Thr and Gly were overrepresented relative to live organism proteins (*49*). This deviation from the general protein composition may be due to a differential degradation of protein components during the diagenesis of the HS.

Incubating Tinker HS in the digestion cocktail without HCl (phenol and thioacetic acid at 110 °C) released very few free amino acids, although a significant quantity of succinate, fumarate, malate, and phosphate or its derivatives were extracted under these conditions (Table 2). It is plausible that the latter components were not in covalent linkages with the rest of the HS; instead they were trapped within the humic matrix and released upon heating. In contrast, the digestion cocktail with 6 or 1 N HCl for 24 h liberated a large quantity of amino acids, which together with the NMR analysis, provided unequivocal evidence that the amino acids were mostly present as peptide residues rather than free forms in Tinker HS. It is possible that this trend may well hold for other humic substances. We are currently applying this approach to other humic substances to test this hypothesis.

Also shown in Table 2, the total nitrogen contributed by the amino acid pool accounted for about 0.5% of the total dry matter in Tinker HS. This is probably an underestimate since it is likely that amino acid recovery from digestion was not complete and that nitrogen from the side chains of Gln and Asn was lost. Taking these factors into account, nitrogen from amino acids constituted a significant fraction (≥22%) of the total N (cf. Table 1) in Tinker HS. However, as a whole, the contribution of peptidic amino acids to Tinker HS dry matter was only 4% (Table 2). Although this percentage may be doubled if recalculated relative to only the carbon mass which was 51% of the total mass (Table 1), the amino acids remain minor components of Tinker HS, which is in agreement with the estimation from FT-IR. Despite this, amino acids dominate the TOCSY cross-peaks in Figure 5. This is readily explained by a higher mobility for the amino acid side groups, compared with other components of Tinker HS in aqueous solution. In turn, this suggests their availability for interactions with dissolved soil constituents such as trace metal nutrients as well as organic and inorganic pollutants. Therefore, in the present case, amino acid residues may have a disproportionately high contribution to humic surface chemistry and properties, even though they may be minor primary structure components.

Conclusions

A California forest soil ("Tinker") used for contaminant bioavailability studies was extracted with NaOH and treated with 4,5-dihydroxy-1,3-benzene disulfonate ("Tiron") to remove exchangeable metal ions. This yielded a humic substance (HS) that was free of Tiron and exhibited improved aqueous solubility at neutral pH (more soil-like). Since no subsequent fractionation and degradative treatments were employed, the resulting product should be closer to whole HS, compared with most other procedures. Element, ash, and FT-IR analyses of Tiron-treated HS indicated a persistent and sizable inorganic fraction, which raised the possibility of organometallic structures or covalently bound mineral fragments in the preparation. This possibility is currently being pursued.

The higher aqueous solubility facilitated extensive analysis of HS by solution-state 2-D ^{1}H and ^{13}C-^{1}H NMR, plus 1-D ^{1}H, ^{13}C, and ^{31}P NMR. The ^{1}H NMR spectra were abundant in amino acids, identified as peptidic from scalar couplings in ^{1}H TOCSY and ^{13}C-^{1}H HSQC as well as dipolar interactions in ^{1}H NOESY. The presence of peptides was independently supported by the FT-IR and py-GCMS analyses plus the release of amino acids only under strongly hydrolyzing conditions. Their identities, principally Gly, Ala, Leu, Ile, Val, Asp, Ser, Thr, Glu, and Pro, were confirmed and quantified by acid digestion of HS followed by 2-D ^{1}H NMR and GCMS analyses. Carbohydrates containing α- and β-pyranoses were also observed in both intact HS and the acid digests. Phosphate mono/diesters, polyphosphates, plus phosphatidic acid esters were evident from ^{1}H NOESY and ^{31}P NMR analysis and were consistent with the high P content from ED-XRF analysis. Methoxyphenylpropanyl structures—possibly derived from lignin residues—were supported by NOESY as well as FT-IR and py-GCMS analyses.

The NOESY, TOCSY, and HSQC together indicated a mobile nature for the peptidic side chains and relatively rigid aromatic groups. Thus the peptidic side chains may be accessible to solvent and water-borne contaminants, while the aromatic groups are probably buried and less accessible. Thus, these approaches in combination contribute to a molecular and dynamic understanding of humic structure—property relations and represent a minimal level of information that needs to be accrued prior to modeling (*50*) of humic structure—property.

Acknowledgments

This work was supported by the U.S. E. P. A. grant #R8259-60010, U.S. E. P. A. funded (#R819658) Center for Ecological Health Research at University of California-Davis, and U.S. Department of Energy grant numbers DE-FG07-96ER20255 and DE-FG03-97ER62349. The NMR spectra were recorded at the MRC Biomedical NMR Centre, Mill Hill. We are grateful to Drs. Egbert Schwartz and Kate Scow for the Tinker soil samples, to Teresa James for her assistance with the FT-IR analysis, and to Dr. David Harris for the natural abundance isotope ratio and C/N analysis.

Literature Cited

(1) Müller-Wegener U. In *Humic Substances and Their Role in the Environment*; Frimmel, F. H., Christman, R. F., Eds.; John Wiley and Sons Ltd.: Chichester, 1988; pp 179—192.
(2) Chapman, D.; Kimstach, V. In *Water Quality Assessments*; Chapman, D., Ed.; Chapman and Hall: London, 1992; p 81.
(3) *Humic Substances in the Global Environment and Implications on Human Health*; Senesi, N., Miano, T. M., Eds.; Elsevier: Amsterdam, 1994; references therein.
(4) Malcolm, R. L. *Anal. Chim. Acta* **1990**, *232*, 19—30.
(5) Preston, C. M. *Soil Sci.* **1996**, *161*, 144—166.
(6) Knicker, H.; Hatcher, P. G. *Naturwissenschaften* **1997**, *84*, 231—234.
(7) *Humic substances II: In Search of structure*; Hayes, M. H. B., MacCarthy, P., Malcolm, R., Swift, R. S., Eds.; Wiley: Chichester, 1989; references therein.
(8) Duxbury, J. M. In *Humic Substances II: In Search of Structure*; Hayes, M. H. B., MacCarthy, P., Malcolm, R., Swift, R. S., Eds.; John Wiley & Sons: Chichester, 1989; pp 594—620.
(9) Stejskal, E. O.; Memory, J. D. *High-Resolution NMR in the Solid State. Fundamentals of CP/MAS*; Oxford University Press: Oxford, 1994.
(10) Wüthrich, K. *NMR of Proteins and Nucleic Acids*; John Wiley and Sons: New York, 1986.
(11) Cavanagh, J. C.; Fairbrother, W. J.; Palmer III, A. G.; Skelton, N. J. *Protein NMR Spectroscopy. Principles and Practice*; Academic Press: San Diego, 1996.
(12) Chien, Y.-Y.; Bleam, W. F. *Environ. Sci. Technol.* **1998**, *32*, 3653—3658
(13) Higashi, R. M.; Fan, T. W.-M.; Lane, A. N. *Analyst* **1998**, *123*, 911—918.
(14) Johnson, C. R.; Scow, K. M. *Biodegradation* **1999**, *10*, 43—50.

(15) Schwartz, E.; Scow, K. M. *Environ. Toxicol. Chem.* **1999**, *18*, 1742−1746.
(16) Schultz, L. F. Ph.D. Thesis, University of California-Davis, 1999.
(17) Davies, G.; Fataftah, A.; Cherkasskiy, A.; Radwan, A.; Jansen, S. A.; Paciolla, M.; Ghabbour, E. A. *Proceedings of the 8th International Humic Substances Society Meeting*; 1994.
(18) Olk, D. C.; Cassman, K. G.; Fan, T. W.-M. *Geoderma* **1995**, *65*, 195−208.
(19) Meltzer, C.; King, B.-S. *Adv. X-ray Anal.* **1991**, *34*, 41−55.
(20) Schagger, H.; von Jagow, G. *Anal. Biochem.* **1987**, *181*, 368−379.
(21) Cherr, G. N.; Fan, T. W. M.; Pillai, M. C.; Shields, T.; Higashi, R. M. *Anal. Biochem.* **1993**, *214*, 521−527.
(22) Stevenson, F.; Goh, K. *Soil Sci.* **1974**, *117*, 34−41.
(23) Schultz, L. F.; Young, T. M.; Higashi, R. M. *Environ. Toxicol. Chem.* **1999**, *18*, 1710−1719.
(24) Moore, S. In *Chemistry and Biology of Peptides*; Ann Arbor Science Publishers: Ann Arbor, 1972; pp 629−653.
(25) Fan, T. W.-M.; Lane, A. N.; Martens, D.; Higashi, R. M. *Analyst* **1998**, *123*, 875−884.
(26) Fan, T. W.-M.; Colmer, T. D.; Lane, A. N.; Higashi, R. M. *Anal. Biochemistry* **1993**, *214*, 260−271
(27) Piotto, M.; Saudek, V.; Sklenar, V. *J. Biomol. Str.* **1992**, *2*, 661−665.
(28) Shaka, A. J.; Keeler, J.; Freeman, R. *J. Magn. Reson.* **1983**, *53*, 313−340.
(29) States, D. J.; Haberkorn, R. A.; Ruben, D. J. *J. Magn. Reson.* **1982**, *48*, 286−292.
(30) Bax, A.; Davis, D. G. *J. Magn. Reson.* **1985**, *65*, 355−360.
(31) Bodenhausen, G.; Ruben, D. J. *Chem. Phys. Lett.* **1980**, *69*, 185−189.
(32) Wishart, D. S.; Bigam, C. G.; Yao, J.; Abildgaard, F.; Dyson, H. J.; Oldfield, E.; Markley, J. L.; Sykes, B. D. *J. Biomolec. NMR* **1995a**, *6*, 135−140.
(33) Gradwell, M. J.; Fan, T. W.-M.; Lane, A. N. *Anal. Biochem.* **1998**, *263*, 139−149.
(34) Davies, B. *Soil Sci. Soc. Am. Proc.* **1974**, *38*, 150−151.
(35) Vance, G. F.; Stevenson, F. J.; Sikora, F. J. In *The Environmental Chemistry of Aluminum*; Sposito, G., Ed.; Lewis Publishers: Boca Raton, 1996; pp 169−220.
(36) Baes, A.; Bloom, P. *Soil Sci. Soc. Am.* **1989**, *53*, 695−700.
(37) Nguyen, T. T.; Janik, L. J.; Raupach, M. *Austr. J. Soil Res.* **1991**, *29*, 49−6.
(38) Faix, O.; Deitrich, M.; Grobe, I. *J. Anal. Appl. Pyrolysis* **1987**, *11*, 403−416.
(39) Schulten, H.; Schnitzer, M. *Soil Sci.* **1992**, *153*, 205−224.
(40) Bracewell, J.; Robertson, G. *J. Soil Sci.* **1976**, *27*, 196−205.
(41) Higashi, R. M.; Fan, T. W.-M.; Lane, A. N. In *Abstracts of the 218th National Meeting of the American Chemical Society*; New Orleans, 1999; p Nucl 44.
(42) Fan, T. W.-M. *Prog. NMR Spectrosc.* **1996**, *28*, 161−219.
(43) Malcolm, R. L. In *Humic Substances II: In Search of Structure*; Hayes, M. H. B., MacCarthy, P., Malcolm, R., Swift, R. S., Eds.; John Wiley & Sons: Chichester, 1989; pp 339−372.
(44) Wishart, D. S.; Bigam, C. G.; Holm, A.; Hodges, R. S.; Sykes, B. D. *J. Biomolec. NMR* **1995b**, *5*, 67−81.
(45) Lane, A. N. *Eur. J. Biochem.* **1989**, *182*, 95−104.
(46) Jokić, A.; Srejić, R.; Pfendt, P. A.; Zakrzewska, J. *Water Air Soil Pollut.* **1995**, *84*, 159−173.
(47) Malcolm, R. L. *Environ. Intl.* **1992**, *18*, 609−620.
(48) Homans, S. W. *A Dictionary of Concepts in NMR*; Clarendon Press: Oxford, 1989.
(49) Handbook for Proteins and peptides. In *Handbook of Biochemistry. Selected data for molecular biology*; Sober, H. A., Ed.; The Chemical Rubber Company: Cleveland, 1970; pp C281−C293.
(50) Sein, L. T., Jr.; Varnum, J. M.; Jansen, S. A. *Environ. Sci. Technol.* **1999**, *33*, 546−552.

Received for review October 1, 1999. Revised manuscript received February 4, 2000. Accepted February 23, 2000.

ES991127V